Hindawi Publishing Corporation
Mathematical Problems in Engineering
Volume 2010, Article ID 627035, 18 pages
doi:10.1155/2010/627035

Research Article

Robust Control of Continuous Bioprocesses

Gongxian Xu

Department of Mathematics, Bohai University, Jinzhou 121000, China

Correspondence should be addressed to Gongxian Xu, dutxugx@yahoo.com.cn

Received 25 March 2010; Revised 17 May 2010; Accepted 5 July 2010

Academic Editor: John Burns

This paper deals with robust control of continuous bioprocesses. According to the material balance equations of continuous bioprocesses, a uniform framework for mathematical modeling of this class of processes is first presented. Then a robust controller is designed by using the H_∞ mixed sensitivity method for the biotechnology processes. The corresponding control objective is described as the development of a robust reference-tracking control structure with the best possible disturbance compensation, able to cope with variations in key process parameters. Finally, the proposed robust control strategy is applied to bio-dissimilation process of glycerol to 1, 3-propanediol. Simulation results are given which show that the designed robust controller makes the system have a favourable robust tracking performance.

1. Introduction

The goal of bioprocess control is to optimize the performance of processes involving industrially important organisms, biomedically relevant species, and the degradation of pollutants [1]. In general, a mathematical model describing the biotechnological process is first needed to do this task. However, it is difficult to obtain its exact process model due to the intrinsic complexity of biological system. Even if the mathematical model is built up, model parameters will vary with the working conditions. In addition, external disturbance signals also have an important effect on the system. These uncertain factors can deteriorate the performance of a bioprocess and lead to the instability of the process. One efficient approach to solving such problems is to design a robust controller via the robust control theory [2–16]. The robust control approach integrates the uncertainty involved in model parameters and external disturbance to synthesize a control law which maintains real plants to work within desired performance specifications despite the effects of uncertainty on the system.

The goals of this work are to represent continuous bioprocesses within an uncertain, linear model framework and to design a robust controller that would perform satisfactorily.

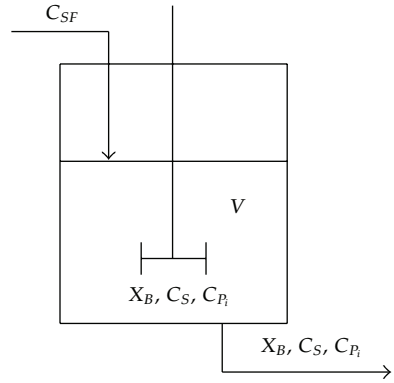

Figure 1: Schematic representation of continuous stirred tank bioreactors.

The corresponding control objective is described as the development of a robust reference-tracking control structure with the best possible disturbance compensation. Simulation results are given which show that the designed robust controller not only ensures the robust stability of the bioprocess in face of the parametric variations in the model, but also makes the system have a favourable robust tracking performance.

In the sequel, we first describe the continuous bioprocesses and present a uniform framework for mathematical modeling of this class of processes. This is followed by a discussion of H_∞ mixed sensitivity approach and selection strategies for weighting functions used to H_∞ design. Then continuous bio-dissimilation of glycerol to 1, 3-propanediol is chosen as a case study and is presented in terms of simulation experiments. Finally, brief conclusions are given in Section 5.

2. Modeling of Continuous Bioprocesses

2.1. Material Balance Equations

The process considered is a continuous stirred tank bioreactor shown in Figure 1. The characteristic of this kind of process is that the reactor is continuously fed with the substrate influent. The rate of outflow is equal to the rate of inflow and the volume of culture remains constant.

The general process model obtained from material balances and conservation laws has the following description:

$$\begin{aligned}
\frac{\mathrm{d}(X_B)}{\mathrm{d}t} &= \mu(C_S, C_{P_1}, C_{P_2}, \ldots, C_{P_n})X_B - DX_B, \\
\frac{\mathrm{d}(C_S)}{\mathrm{d}t} &= D(C_{SF} - C_S) - q_S(C_S, C_{P_1}, C_{P_2}, \ldots, C_{P_n})X_B, \\
\frac{\mathrm{d}(C_{P_i})}{\mathrm{d}t} &= q_{P_i}(C_S, C_{P_1}, C_{P_2}, \ldots, C_{P_n}, D)X_B - DC_{P_i}, \quad i = 1, 2, \ldots, n,
\end{aligned} \tag{2.1}$$

where C_{SF} is the external substrate concentration; D is the dilution rate; X_B, C_S, and C_{P_i} are

the concentrations of biomass, substrate, and product P_i, respectively; μ, q_S, and q_{P_i} are the specific growth rate of cells, specific consumption rate of substrate, specific formation rate of product P_i, respectively. In general μ and q_S are the functions of substrate concentration C_S and product concentrations C_{P_i}. But for the specific formation rate q_{P_i}, its expression is a function of substrate concentration C_S, product concentrations C_{P_i}, and dilution rate D (e.g., the specific formation rate of product ethanol in bio-dissimilation process of glycerol to 1, 3-propanediol, see Section 4).

2.2. Control Model of Continuous Bioprocesses

The process dynamics (2.1) is represented as a linear model with uncertain parameters

$$\begin{aligned} \dot{x} &= A(\theta)x + B(\theta)u, \\ y &= Cx, \end{aligned} \tag{2.2}$$

where $x = (X_B, C_S, C_{P_1}, C_{P_2}, \ldots, C_{P_n})^{\mathrm{T}} \in R^{n+2}$ is used for the vector of states, $u = D$ is the control input, $y = C_S$ is the measured output, $\theta = (X_B, C_S, C_{P_1}, C_{P_2}, \ldots, C_{P_n}, D)^{\mathrm{T}} \in R^{n+3}$ is a vector of describing uncertain parameters, and

$$A(\theta) = \begin{bmatrix} \mu(\theta_2, \theta_3, \ldots, \theta_{n+2}) & 0 & 0 & \cdots & 0 \\ -q_S(\theta_2, \theta_3, \ldots, \theta_{n+2}) & 0 & 0 & \cdots & 0 \\ q_{P_1}(\theta_2, \theta_3, \ldots, \theta_{n+3}) & 0 & 0 & \cdots & 0 \\ \vdots & \vdots & \vdots & \ddots & \vdots \\ q_{P_n}(\theta_2, \theta_3, \ldots, \theta_{n+3}) & 0 & 0 & \cdots & 0 \end{bmatrix}, \quad B(\theta) = \begin{bmatrix} -\theta_1 \\ C_{SF} - \theta_2 \\ -\theta_3 \\ \vdots \\ -\theta_{n+2} \end{bmatrix}, \quad C = \begin{bmatrix} 0 \\ 1 \\ 0 \\ \vdots \\ 0 \end{bmatrix}^{\mathrm{T}}. \tag{2.3}$$

The specific growth rate of cells (μ), specific consumption rate of substrate (q_S), and specific formation rate of product P_i(q_{P_i}) will change within certain ranges due to variations in the working conditions. In other words, all parameters in $A(\theta)$ and $B(\theta)$ are accepted to vary within known bounds.

Considering all the uncertain parameters in θ, we allow their changes of up to H_k% ($0 < H_k \leq 100$, $k = 1, 2, \ldots, n+3$) around the nominal values, respectively. Then all uncertain parameters can be uniformly denoted as

$$\theta = (I + H\Delta)\theta_0, \tag{2.4}$$

where $\theta_0 = (X_{B0}, C_{S0}, C_{P_10}, C_{P_20}, \ldots, C_{P_n0}, D_0)^{\mathrm{T}}$ is the nominal value of vector θ, I is the identity

matrix, and H and Δ are the diagonal matrices with the following formulations:

$$H = \begin{bmatrix} H_1 & & & \\ & H_2 & & \\ & & \ddots & \\ & & & H_{n+3} \end{bmatrix}, \qquad \Delta = \begin{bmatrix} \Delta_1 & & & \\ & \Delta_2 & & \\ & & \ddots & \\ & & & \Delta_{n+3} \end{bmatrix}, \tag{2.5}$$

where $|\Delta_k| \le 1$ $(k = 1, 2, \ldots, n+3)$.

The following Theorem 2.1 provides a uniform framework for mathematical modeling of continuous bioprocesses.

Theorem 2.1. *The transfer function model for continuous bioprocesses can be formulated uniformly as*

$$G_P(s) = 1. \tag{2.6}$$

Proof. For $\theta_k \in [\theta_{0k}(1 - H_k), \theta_{0k}(1 + H_k)]$, the transfer function of the process can be derived as

$$\begin{aligned} G_P(s) &= C(sI - A(\theta))^{-1}B(\theta) \\ &= \begin{bmatrix} 0 \\ 1 \\ 0 \\ \vdots \\ 0 \end{bmatrix}^{\mathrm{T}} \left(\begin{bmatrix} s & & & & \\ & s & & & \\ & & s & & \\ & & & \ddots & \\ & & & & s \end{bmatrix} - \begin{bmatrix} \mu & 0 & 0 & \cdots & 0 \\ -q_S & 0 & 0 & \cdots & 0 \\ q_{P_1} & 0 & 0 & \cdots & 0 \\ \vdots & \vdots & \vdots & \ddots & \vdots \\ q_{P_n} & 0 & 0 & \cdots & 0 \end{bmatrix} \right)^{-1} \begin{bmatrix} -\theta_1 \\ C_{SF} - \theta_2 \\ -\theta_3 \\ \vdots \\ -\theta_{n+2} \end{bmatrix} \\ &= \begin{bmatrix} 0 \\ 1 \\ 0 \\ \vdots \\ 0 \end{bmatrix}^{\mathrm{T}} \begin{bmatrix} s - \mu(\theta_2, \theta_3, \ldots, \theta_{n+2}) & 0 & 0 & \cdots & 0 \\ q_S(\theta_2, \theta_3, \ldots, \theta_{n+2}) & s & 0 & \cdots & 0 \\ -q_{P_1}(\theta_2, \theta_3, \ldots, \theta_{n+3}) & 0 & s & \cdots & 0 \\ \vdots & \vdots & \vdots & \ddots & \vdots \\ -q_{P_n}(\theta_2, \theta_3, \ldots, \theta_{n+3}) & 0 & 0 & \cdots & s \end{bmatrix}^{-1} \begin{bmatrix} -\theta_1 \\ C_{SF} - \theta_2 \\ -\theta_3 \\ \vdots \\ -\theta_{n+2} \end{bmatrix} \\ &= \begin{bmatrix} 0 \\ 1 \\ 0 \\ \vdots \\ 0 \end{bmatrix}^{\mathrm{T}} \begin{bmatrix} \dfrac{1}{s - \mu(\theta_2, \theta_3, \ldots, \theta_{n+2})} & 0 & 0 & \cdots & 0 \\ \dfrac{-q_S(\theta_2, \theta_3, \ldots, \theta_{n+2})}{s(s - \mu(\theta_2, \theta_3, \ldots, \theta_{n+2}))} & \dfrac{1}{s} & 0 & \cdots & 0 \\ \dfrac{q_{P_1}(\theta_2, \theta_3, \ldots, \theta_{n+3})}{s(s - \mu(\theta_2, \theta_3, \ldots, \theta_{n+2}))} & 0 & \dfrac{1}{s} & \cdots & 0 \\ \vdots & \vdots & \vdots & \ddots & \vdots \\ \dfrac{q_{P_n}(\theta_2, \theta_3, \ldots, \theta_{n+3})}{s(s - \mu(\theta_2, \theta_3, \ldots, \theta_{n+2}))} & 0 & 0 & \cdots & \dfrac{1}{s} \end{bmatrix} \begin{bmatrix} -\theta_1 \\ C_{SF} - \theta_2 \\ -\theta_3 \\ \vdots \\ -\theta_{n+2} \end{bmatrix} \\ &= \frac{q_S(\theta_2, \theta_3, \ldots, \theta_{n+2})\theta_1 + (C_{SF} - \theta_2)(s - \mu(\theta_2, \theta_3, \ldots, \theta_{n+2}))}{s(s - \mu(\theta_2, \theta_3, \ldots, \theta_{n+2}))}. \end{aligned} \tag{2.7}$$

Replacing θ_1 and θ_2 with X_B and C_S, respectively, we have

$$G_P(s) = \frac{q_S X_B + (C_{SF} - C_S)(s-\mu)}{s(s-\mu)}. \tag{2.8}$$

This model describes the transfer functions of continuous bioprocesses for all uncertain parameters $\theta_k \in [\theta_{0k}(1 - H_k), \theta_{0k}(1 + H_k)]$. □

In this paper, we choose the multiplicative form of uncertainty modeling to represent the relative error in the process model

$$G_P(s) = G_{P0}(s)(1 + \Delta_m(s)), \tag{2.9}$$

where

$$G_{P0}(s) = \frac{q_S X_{B0} + (C_{SF} - C_{S0})(s-\mu)}{s(s-\mu)} \tag{2.10}$$

is the nominal model of the plant, and

$$\Delta_m = \frac{G_P(s) - G_{P0}(s)}{G_{P0}(s)}. \tag{2.11}$$

3. H_∞ Mixed Sensitivity Method

3.1. H_∞ Mixed Sensitivity Problem

The H_∞ mixed sensitivity problem is formulated as the one of finding a feedback controller that stabilizes the closed-loop system shown in Figure 2 and minimizes the H_∞-norm of closed-loop transfer function T_{zw} from the exogenous input w ($w = r$) to the regulated outputs z ($z = [z_1, z_2, z_3]^T$), namely,

$$\gamma_{\text{opt}} = \min_K \|T_{zw}(s)\|_\infty, \tag{3.1}$$

where

$$T_{zw}(s) = \begin{bmatrix} W_1(s)S(s) \\ W_2(s)K(s)S(s) \\ W_3(s)T(s) \end{bmatrix} = P_{11}(s) + P_{12}(s)K(s)(I - P_{22}(s)K(s))^{-1}P_{21}(s). \tag{3.2}$$

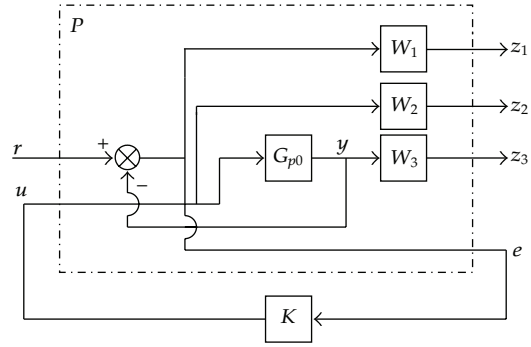

Figure 2: Mixed sensitivity configuration.

Here $S(s) = (I + G_{p0}(s)K(s))^{-1}$, $K(s)S(s)$, and $T(s) = G_{p0}(s)K(s)S(s)$ are the sensitivity transfer matrix, control sensitivity transfer matrix, and complementary sensitivity transfer matrix, respectively; $G_{p0}(s)$ is the nominal model that has no imaginary axis zeros and/or poles; the terms $W_1(s)$, $W_2(s)$, and $W_3(s)$ are performance weighting function, control weighting function, and robustness weighting function, respectively; $P(s)$ is the augmented plant and can be denoted as

$$P(s) = \left[\begin{array}{c|c} P_{11} & P_{12} \\ \hline P_{21} & P_{22} \end{array}\right] = \left[\begin{array}{c|c} W_1 & -W_1 G_{p0} \\ 0 & W_2 \\ 0 & W_3 G_{p0} \\ \hline I & -G_{p0} \end{array}\right] \tag{3.3}$$

with state-space realization

$$P(s) = \left[\begin{array}{c|cc} A_p & B_1 & B_2 \\ \hline C_1 & D_{11} & D_{12} \\ C_2 & D_{21} & D_{22} \end{array}\right] \tag{3.4}$$

For the H_∞ optimal control problem (3.1), all assumptions concerning the existence of a solution $K(s)$ are satisfied [2, 3].

(a) The pair (A_p, B_2) is stabilizable and (A_p, C_2) is detectable.

(b) $\operatorname{rank}(D_{12}) = \dim(u)$ and $\operatorname{rank}(D_{21}) = \dim(y)$.

(c) The following matrices must have full rank for

$$\begin{bmatrix} A_p - j\omega I & B_2 \\ C_1 & D_{12} \end{bmatrix}, \quad \begin{bmatrix} A_p - j\omega I & B_1 \\ C_2 & D_{21} \end{bmatrix}, \quad \forall \omega \in R. \tag{3.5}$$

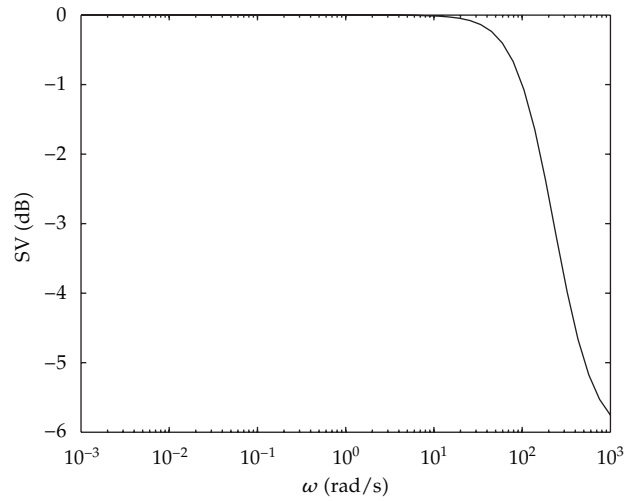

Figure 3: Singular values Bode plot of cost functions T_{zw}.

Assumption (a) ensures the stability of a synthesized H_∞ controller. The second assumption guarantees that the designed H_∞ controller is a proper and real rational function. The final assumption is a mathematical technicality that enables both $P_{12}(s)$ and $P_{21}(s)$ to have no invariant zeros on the imaginary axis [6].

3.2. Weighting Function Selection

The selection of the weighting functions $W_1(s)$, $W_2(s)$, and $W_3(s)$ keeps mainly to the basic rules as follows.

(a) Choose a low-order weighting function, otherwise a high-order H_∞ controller can be achieved.

(b) As the perturbation bound of the uncertainty Δ_m, the choice of robustness weighting function $W_3(s)$ depends also on whether the nominal model is strictly proper and real rational function. Usually, $W_3(s)$ is chosen to be an improper and real rational function because the most system in the world is strictly proper. Though $W_3(s)$ cannot be realized in state-space form, $W_3(s)G_{P0}(s)$ has a state-space realization since it is a proper structure. This ensures D_{12} has a full rank.

(c) The performance weighting function $W_1(s)$ is usually a stable, proper, and real rational function. The 0 dB crossover frequency for the Bode plot of $W_1(s)$ should be below the 0 dB crossover frequency for the Bode plot of $W_3(s)$. More precisely, for all $\omega \in R$, we require $\overline{\sigma}(W_1^{-1}(j\omega)) + \overline{\sigma}(W_3^{-1}(j\omega)) > 1$, where $\overline{\sigma}$ denotes the maximum singular value of a transfer function.

(d) The control weighting function $W_2(s)$ is normally chosen to be a high-pass filter to penalize the control signal and to ensure that the D_{12} submatrix of state-space representation of the augmented plant $P(s)$ has full column rank. It is also included in this paper to limit the size of the controller gain.

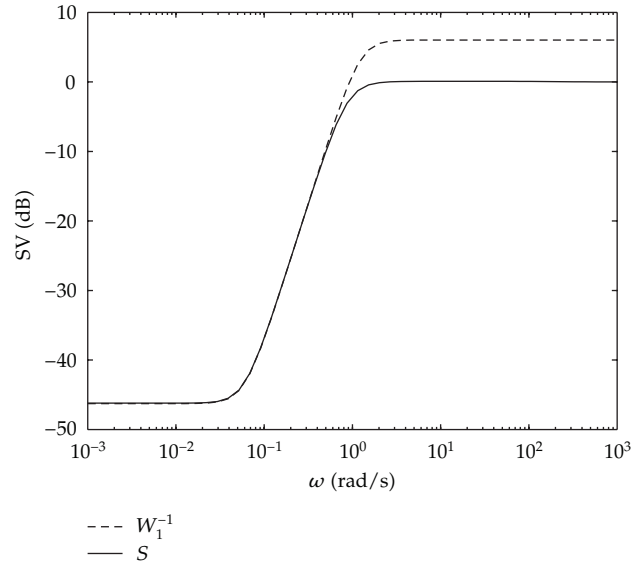

Figure 4: Singular values Bode plots of S and $W_1^{-1}(s)$.

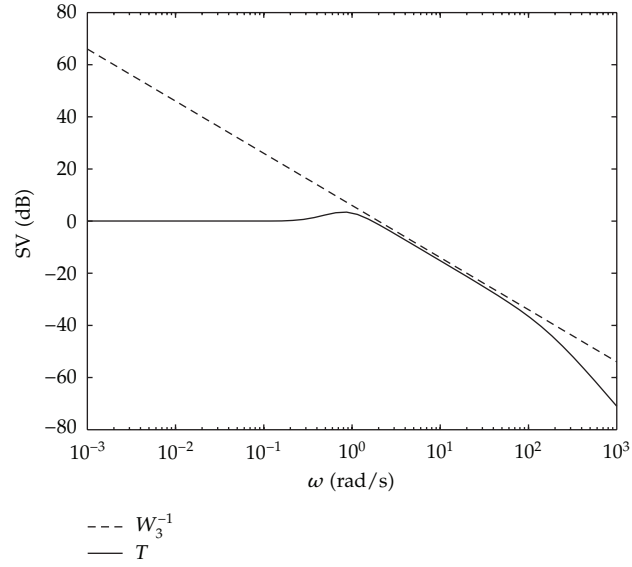

Figure 5: Singular values Bode plots of T and $W_3^{-1}(s)$.

4. Case Study

In this section, we study the robust control of continuous bio-dissimilation of glycerol to 1, 3-propanediol.

In the bioconversion of glycerol to 1, 3-propanediol, a number of products may be simultaneously produced, depending on the microorganisms and conditions used. Under

Table 1: Parameters in the models (4.3)–(4.5).

Substrate/products	m	Y^m	Δq^m	K^*
Glycerol	2.20	0.0082	28.58	11.43
1, 3-propanediol	–2.69	67.69	26.59	15.50
Acetic acid	–0.97	33.07	5.74	85.71

proper fermentation conditions mainly 1, 3-propanediol, acetic acid and ethanol are formed. The material balance equations of continuous microbial cultures are written as follows [17]:

$$\begin{aligned}
\frac{dX}{dt} &= (\mu - D)X, \\
\frac{dC_S}{dt} &= D(C_{SF} - C_S) - q_S X, \\
\frac{dC_{PD}}{dt} &= q_{PD}X - DC_{PD}, \\
\frac{dC_{HAc}}{dt} &= q_{HAc}X - DC_{HAc}, \\
\frac{dC_{EtOH}}{dt} &= q_{EtOH}X - DC_{EtOH},
\end{aligned} \tag{4.1}$$

where X is the biomass, g/L; D is the dilution rate, 1/h; C_{SF} and C_S are the substrate concentration (glycerol) in feed and reactor, respectively, mmol/L; C_{PD}, C_{HAc}, and C_{EtOH} are the concentrations of products 1,3-propanediol, acetic acid, and ethanol, respectively, mmol/L; t is the fermentation time, h; μ,q_S,q_{PD},q_{HAc} and q_{EtOH} are the specific growth rate of cells, specific consumption rate of substrate, specific formation rate of products 1,3-propanediol, acetic acid and ethanol, respectively, mmol/gh, which can be expressed as:

$$\mu = \mu_m \frac{C_S}{K_S + C_S}\left(1 - \frac{C_S}{C_S^*}\right)\left(1 - \frac{C_{PD}}{C_{PD}^*}\right)\left(1 - \frac{C_{HAc}}{C_{HAc}^*}\right)\left(1 - \frac{C_{EtOH}}{C_{EtOH}^*}\right), \tag{4.2}$$

$$q_S = m_S + \frac{\mu}{Y_S^m} + \Delta q_S^m \frac{C_S}{C_S + K_S^*}, \tag{4.3}$$

$$q_{PD} = m_{PD} + \mu Y_{PD}^m + \Delta q_{PD}^m \frac{C_S}{C_S + K_{PD}^*}, \tag{4.4}$$

$$q_{HAc} = m_{HAc} + \mu Y_{HAc}^m + \Delta q_{HAc}^m \frac{C_S}{C_S + K_{HAc}^*}, \tag{4.5}$$

$$q_{EtOH} = q_S\left(\frac{b_1}{c_1 + DC_S} + \frac{b_2}{c_2 + DC_S}\right). \tag{4.6}$$

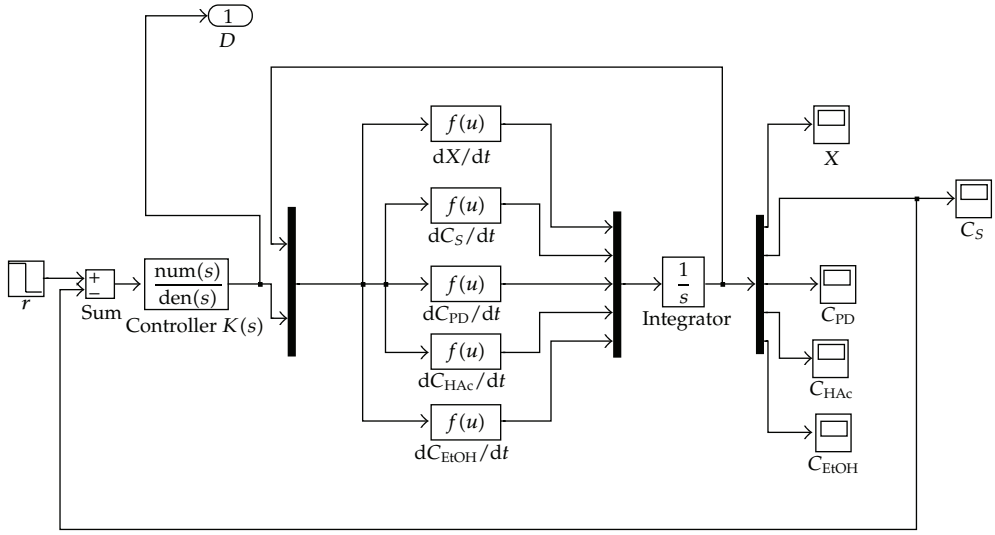

Figure 6: Simulation model of the nonlinear bioprocess.

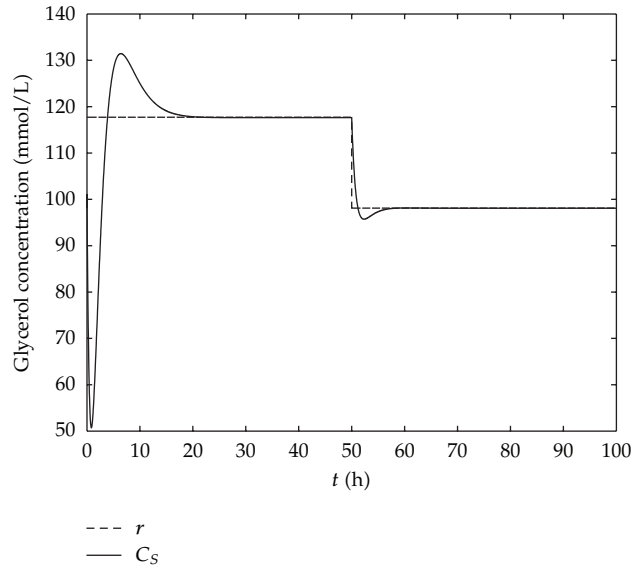

Figure 7: Output (glycerol concentration) response.

For *Klebsiella pneunoniae* cultivated under anaerobic conditions at 37°C and pH 7.0, the maximum specific growth rate μ_m and the saturation constant for glycerol present the values of 0.67 1/h and 0.28 mmol/L, respectively. The critical concentrations denoted as C^* in glycerol, 1, 3-propanediol, acetic acid, and ethanol are 2039, 939.5, 1026, and 360.9 mmol/L, respectively. In addition, the parameters b_1, b_2, c_1, and c_2 in (4.6) are 0.025, 5.18, 0.06, and 50.45 mmol/Lh, respectively, while the ones for (4.3), (4.4) and (4.5) are listed in Table 1.

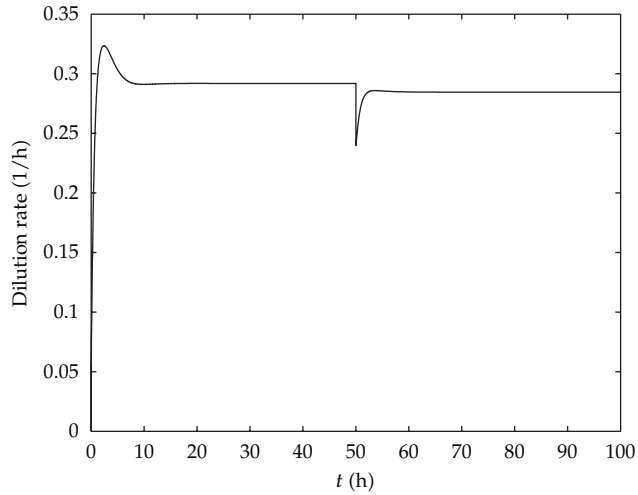

Figure 8: Time trajectory of dilution rate.

The process dynamics (4.1) is represented as a linear model with uncertain parameters:

$$\begin{aligned} \dot{x} &= Ax + Bu, \\ y &= Cx, \end{aligned} \tag{4.7}$$

where $x = (X, C_S, C_{\mathrm{PD}}, C_{\mathrm{HAc}}, C_{\mathrm{EtOH}})^{\mathrm{T}}$ is used for the vector of states, $u = D$ is the control input, $y = C_S$ is the measured output,

$$A = \begin{bmatrix} \mu & 0 & 0 & 0 & 0 \\ -q_S & 0 & 0 & 0 & 0 \\ q_{\mathrm{PD}} & 0 & 0 & 0 & 0 \\ q_{\mathrm{HAc}} & 0 & 0 & 0 & 0 \\ q_{\mathrm{EtOH}} & 0 & 0 & 0 & 0 \end{bmatrix}, \quad B = \begin{bmatrix} -X \\ C_{SF} - C_S \\ -C_{\mathrm{PD}} \\ -C_{\mathrm{HAc}} \\ -C_{\mathrm{EtOH}} \end{bmatrix}, \quad C = \begin{bmatrix} 0 \\ 1 \\ 0 \\ 0 \\ 0 \end{bmatrix}^{\mathrm{T}}. \tag{4.8}$$

By Theorem 2.1, the process transfer function can be derived as

$$G_p(s) = \frac{(C_{SF} - C_S)s + q_S X - \mu(C_{SF} - C_S)}{s(s - \mu)}. \tag{4.9}$$

The initial glycerol concentration C_{SF} is set to be 730.8 mmol/L. The variable numerical data for the example are given in Table 2. The plant's nominal model in a transfer function form is

Table 2: Variable numerical data.

Data	Nominal values	Variation bounds	
		Min	Max
D (1/h)	0.2857	0	$2\,D_0$
X (g/L)	2.89	$0.75\,X_0$	$1.25\,X_0$
C_S (mmol/L)	98.1	$0.4\,C_{S0}$	$1.6\,C_{S0}$
C_{PD} (mmol/L)	400.1	$0.75\,C_{PD0}$	$1.25\,C_{PD0}$
C_{HAc} (mmol/L)	116.6	$0.75\,C_{HAc0}$	$1.25\,C_{HAc0}$
C_{EtOH} (mmol/L)	42.33	$0.75\,C_{EtOH0}$	$1.25\,C_{EtOH0}$

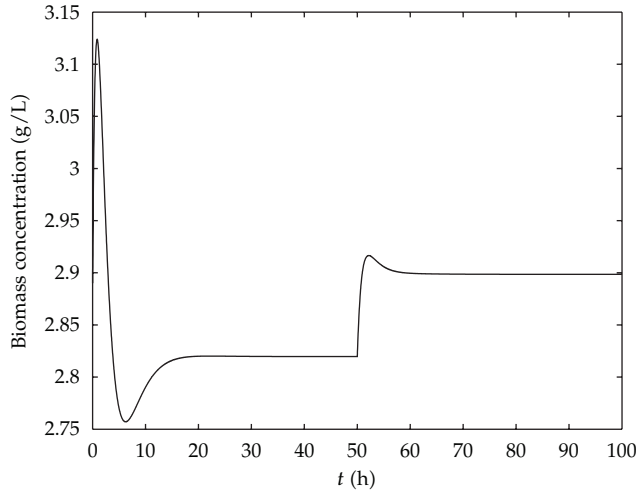

Figure 9: Time trajectory of biomass concentration.

expressed as

$$G_0(s) = \frac{632.7}{s - 0.2857}. \tag{4.10}$$

Based on the previously-mentioned rules concerning the choice of the weighting function, robustness weighting function $W_3(s)$ can be chosen as $W_3(s) = s/2$ whose crossover frequency is $\omega_{c3} = 2\,\text{rad/s}$; performance weighting function $W_1(s)$ is a second-order filter with

$$W_1(s) = \frac{\beta\left(\alpha s^2 + 2\zeta_1\omega_{c1}\sqrt{\alpha}s + \omega_{c1}^2\right)}{\beta s^2 + 2\zeta_2\omega_{c1}\sqrt{\beta}s + \omega_{c1}^2}, \tag{4.11}$$

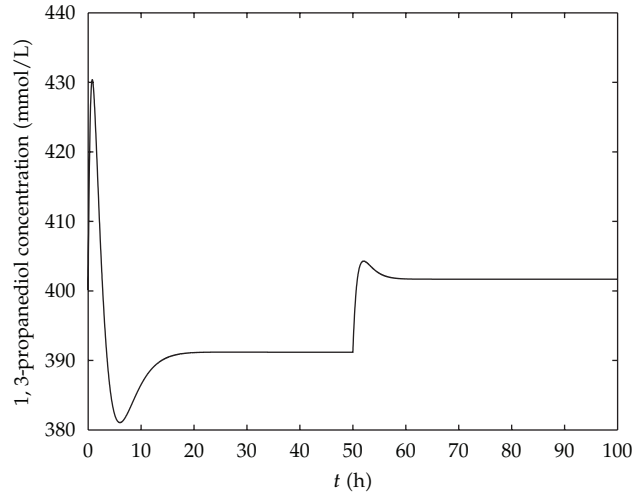

Figure 10: Time trajectory of 1, 3-propanediol concentration.

where $\beta = 206$: DC gain of the filter (controls the disturbance rejection); $\alpha = 0.5$: high frequency gain (controls the response peak overshoot); $\omega_{c1} = 0.865\,\text{rad/s}$: filter crossover frequency; $\zeta_1 = 0.6$, $\zeta_2 = 0.7$: damping ratios of the corner frequencies. Obviously, $W_1^{-1}(0) = 1/\beta$ is the steady-state tracking error, and $\lim_{s\to\infty} W_1^{-1}(s) = 1/\alpha = 2$ is the corresponding amplification factor of the high-frequency disturbances. The weighting function $W_2(s)$ is selected as $W_2(s) = 0.1$.

By using MATLAB, the augmented plant $P(s)$ has the following state-space realization:

$$A_p = \begin{bmatrix} 0.2857 & 0 & 0 \\ -632.7 & -0.0852 & -0.0036 \\ 0 & 1.0000 & 0 \end{bmatrix}, \quad B_1 = \begin{bmatrix} 0 \\ 1 \\ 0 \end{bmatrix}, \quad B_2 = \begin{bmatrix} 1 \\ 0 \\ 0 \end{bmatrix},$$

$$C_1 = \begin{bmatrix} -316.35 & 0.8137 & 0.7464 \\ 0 & 0 & 0 \\ 90.3812 & 0 & 0 \end{bmatrix}, \quad C_2 = \begin{bmatrix} -632.7 & 0 & 0 \end{bmatrix}, \tag{4.12}$$

$$D_{11} = \begin{bmatrix} 0.5 \\ 0 \\ 0 \end{bmatrix}, \quad D_{12} = \begin{bmatrix} 0 \\ 0.1000 \\ 316.35 \end{bmatrix}, \quad D_{21} = 1, \quad D_{22} = 0.$$

After 9 iterations, γ_{opt} is found to be 0.99. The corresponding H_∞ controller is stable and has

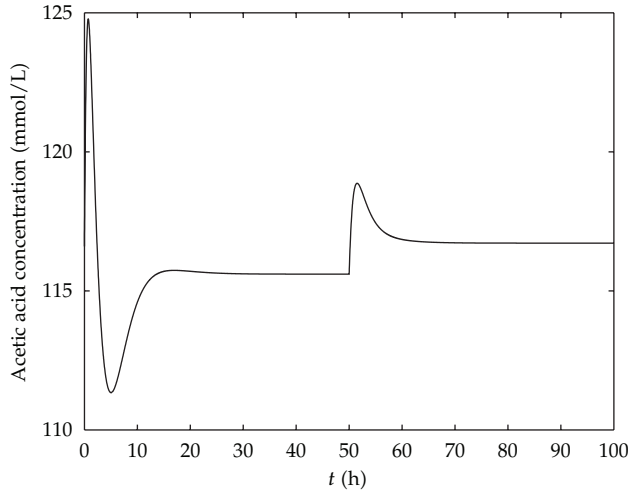

Figure 11: Time trajectory of acetic acid concentration.

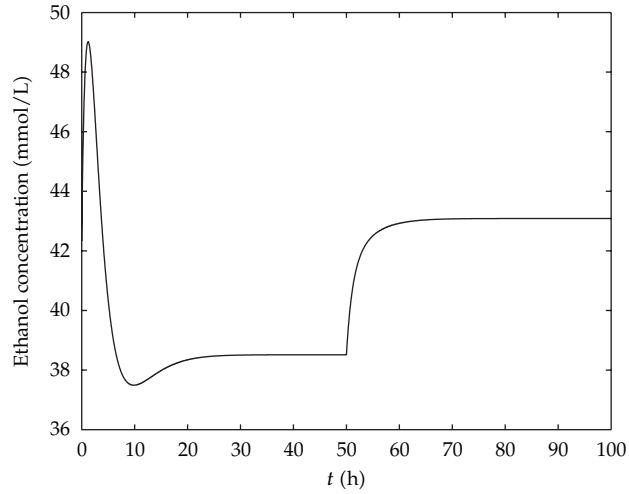

Figure 12: Time trajectory of ethanol concentration.

the same number of states as the augmented plant with transfer function

$$K(s) = \frac{0.4511s^2 + 0.2927s + 0.05571}{s^3 + 165.5s^2 + 14.1s + 0.6006}. \tag{4.13}$$

The closed-loop poles are -163.5625, $-0.6251 + 0.6028i$, $-0.6251 - 0.6028i$, -0.2843, $-0.0426 + 0.0426i$, and $-0.0426 - 0.0426i$, respectively.

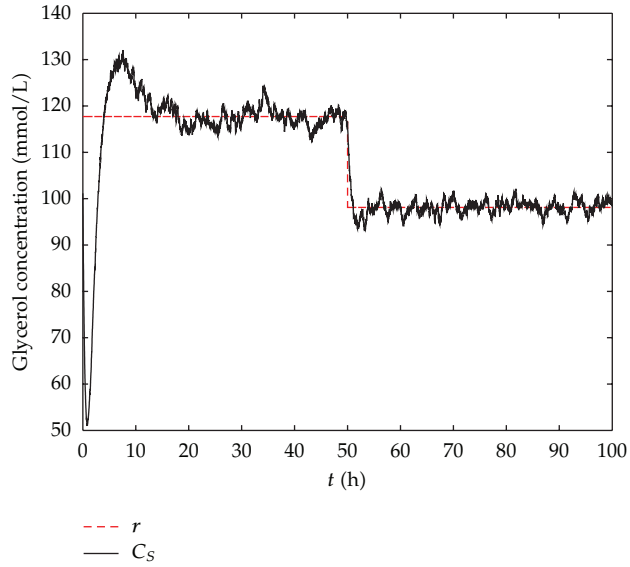

Figure 13: Output (glycerol concentration) response in the presence of noise.

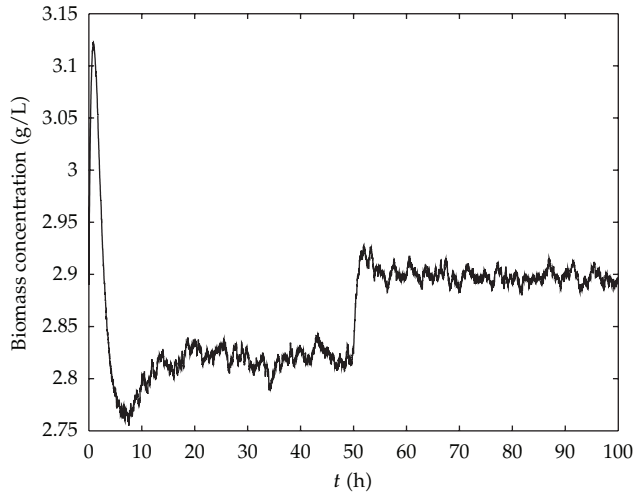

Figure 14: Time trajectory of biomass concentration in the presence of noise.

Figure 3 shows the singular value Bode plot of cost function $T_{zw}(s)$. As shown, the cost function $T_{zw}(s)$ is all-pass, that is, $\overline{\sigma}(T_{zw}(j\omega)) = 1$ hold for all $\omega \in R$. The results of the singular values analysis for the sensitivity function $S(s)$, the complementary sensitivity function $T(s)$, and their associated weighting functions $W_1^{-1}(s)$ and $W_3^{-1}(s)$ are illustrated in Figures 4 and 5. It can be observed that S is below its upper bound W_1^{-1} at a low frequency whereas T locates below its upper bound W_3^{-1} at a high frequency, that is, $\overline{\sigma}(S(j\omega)) \leq W_1^{-1}(j\omega)$ and $\overline{\sigma}(T(j\omega)) \leq W_3^{-1}(j\omega)$ hold. These results not only indicate that the closed-loop system has a favourable performance of disturbance reduction but also guarantee the robust stability of controlled system in face of the parametric uncertainty in model.

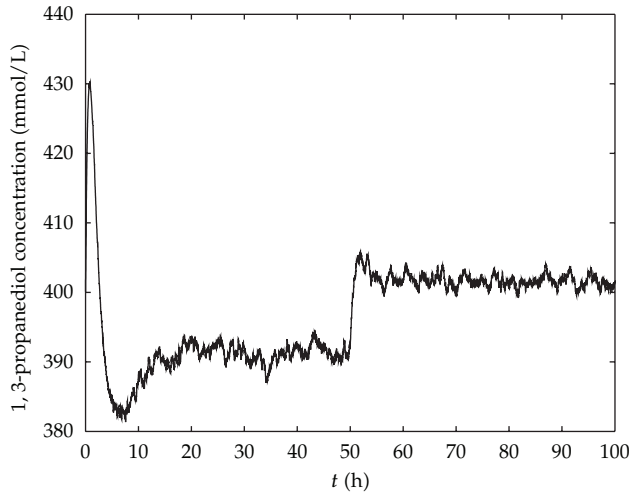

Figure 15: Time trajectory of 1, 3-propanediol concentration in the presence of noise.

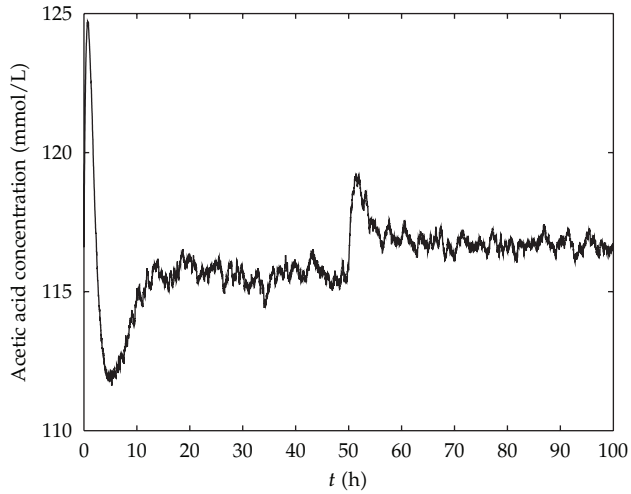

Figure 16: Time trajectory of acetic acid concentration in the presence of noise.

Tests of controller performance were carried out through simulation of the whole nonlinear system employing MATLAB/SIMULINK. The complete simulation model is shown in Figure 6. The numerical integration of the nonlinear equations (4.1) is based on the 5th-order Runge-Kutta method. In the simulation experiments, we consider a reference input as follows:

$$r(t) = \begin{cases} 98.1(1 + 0.2), & 0 \le t < 50, \\ 98.1, & 50 \le t \le 100. \end{cases} \tag{4.14}$$

Then the dynamic response curve of the substrate concentration is plotted in Figure 7. From Figure 7, it can be seen that the substrate concentration C_S tracks favourably the reference

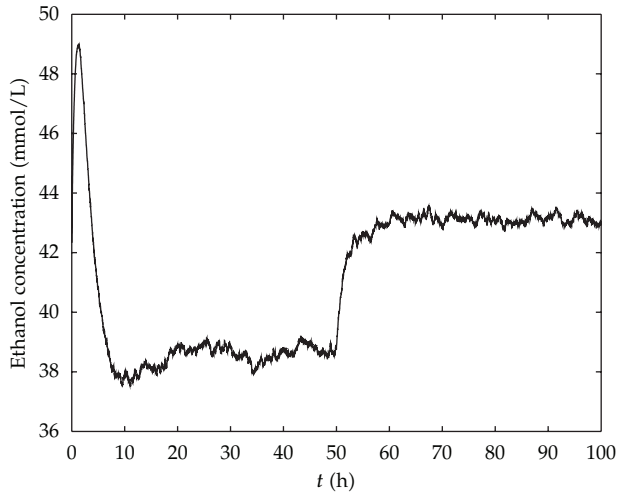

Figure 17: Time trajectory of ethanol concentration in the presence of noise.

input r. The results imply that the H_∞ controller $K(s)$ has a good control action on the presented bioprocess. The time trajectories of the dilution rate, the biomass concentration, and the concentrations of 1, 3-propanediol, acetic acid, and ethanol are presented in Figures 8, 9, 10, 11, and 12. The dynamic trajectories of all variable data stay within the operation ranges as specified in Table 2.

To detect the dynamic tracking performance of the system in the presence of noise measurement, an additive white Gaussian noise with variance $0.05C_S$ is added in the simulations. The simulation results are shown in Figures 13, 14, 15, 16, and 17. As shown in Figures 13–17, the substrate concentration tracks favourably the reference signal. While the time trajectories of other variables stay within the operation windows as given in Table 2.

5. Conclusions

This paper has presented a uniform modeling framework and robust control design for continuous bioprocesses. By taking into account the uncertainties in the model parameters, we have first developed the uncertain, linear state-space model of continuous bioprocesses. Then a uniform transfer function model is derived. In the H_∞ controller design, a scalar weighting matrix W_2 on the control input to the plant has been used to limit the size of the controller gain. Our work has demonstrated that the designed robust controller not only ensures the robust stability of the bioprocess in face of the parametric variations in the model, but also makes the system has a favourable robust tracking performance in the presence of set-point variations.

References

[1] E. Carson, D. D. Feng, M.-N. Pons, R. Soncini-Sessa, and G. van Straten, "Dealing with bio- and ecological complexity: challenges and opportunities," *Annual Reviews in Control*, vol. 30, no. 1, pp. 91–101, 2006.

[2] J. C. Doyle, K. Glover, P. P. Khargonekar, and B. A. Francis, "State-space solutions to standard $\mathscr{H}_2$ and $\mathscr{H}_\infty$ control problems," *IEEE Transactions on Automatic Control*, vol. 34, no. 8, pp. 831–847, 1989.

[3] S. Skogestad and I. Postlethwaite, *Multivariable Feedback Control: Analysis and Design*, Wiley, New York, NY, USA, 1996.
[4] G. E. Dullerud and F. Paganini, *A Course in Robust Control Theory: A Convex Approach*, Springer, Berlin, Germany, 2000.
[5] I. R. Petersen, V. A. Ugrinovskii, and A. V. Savkin, *Robust Control Design Using H_∞-Methods*, Communications and Control Engineering Series, Springer, London, UK, 2000.
[6] X. P. Li, B. C. Chang, S. S. Banda, and H. H. Yeh, "Robust control systems design using H_∞ optimization theory," *Journal of Guidance, Control, and Dynamics*, vol. 15, no. 4, pp. 944–952, 1992.
[7] M. G. Ortega and F. R. Rubio, "Systematic design of weighting matrices for the H_∞ mixed sensitivity problem," *Journal of Process Control*, vol. 14, no. 1, pp. 89–98, 2004.
[8] R. S. Parker, F. J. Doyle III, J. H. Ward, and N. A. Peppas, "Robust H_∞ glucose control in diabetes using a physiological model," *AIChE Journal*, vol. 46, no. 12, pp. 2537–2549, 2000.
[9] E. Ruiz-Velázquez, R. Femat, and D. U. Campos-Delgado, "Blood glucose control for type I diabetes mellitus: a robust tracking H_∞ problem," *Control Engineering Practice*, vol. 12, no. 9, pp. 1179–1195, 2004.
[10] E. Elisante, G. P. Rangaiah, and S. Palanki, "Robust controller synthesis for multivariable nonlinear systems with unmeasured disturbances," *Chemical Engineering Science*, vol. 59, no. 5, pp. 977–986, 2004.
[11] P. G. Georgieva and S. Feyo De Azevedo, "Robust control design of an activated sludge process," *International Journal of Robust and Nonlinear Control*, vol. 9, no. 13, pp. 949–967, 1999.
[12] S. Stoyanov and I. Simeonov, "Robust compensator control of continuous fermentation processes," *Bioprocess and Biosystems Engineering*, vol. 15, no. 6, pp. 295–300, 1996.
[13] T. T. Lee, F. Y. Wang, and R. B. Newell, "Robust multivariable control of complex biological processes," *Journal of Process Control*, vol. 14, no. 2, pp. 193–209, 2004.
[14] S. K. Nguang and X. D. Chen, "Robust $\mathscr{H}_\infty$ control of a class of continuous fermentation processes," *Applied Mathematics Letters*, vol. 12, no. 6, pp. 61–69, 1999.
[15] F. Renard, A. V. Wouwer, S. Valentinotti, and D. Dumur, "A practical robust control scheme for yeast fed-batch cultures—an experimental validation," *Journal of Process Control*, vol. 16, no. 8, pp. 855–864, 2006.
[16] G. Quiroz and R. Femat, "Theoretical blood glucose control in hyper- and hypoglycemic and exercise scenarios by means of an H_∞ algorithm," *Journal of Theoretical Biology*, vol. 263, no. 1, pp. 154–160, 2010.
[17] Z. L. Xiu, A.-P. Zeng, and L. J. An, "Mathematical modeling of kinetics and research on multiplicity of glycerol bioconversion to 1, 3-propanediol," *Journal of Dalian University of Technology*, vol. 40, no. 4, pp. 428–433, 2000.